Doppler Frequency Estimators under Additive and Multiplicative Noise

Aaron C. Chan[a], Edmund Y. Lam[a], and Vivek J. Srinivasan[b,c]

[a]Department of Electrical and Electronic Engineering, Pokfulam Road, The University of Hong Kong, Hong Kong;
[b]Biomedical Engineering Department, UC Davis, 451 Health Sciences Drive, Davis, CA 95616, USA;
[c]MGH/MIT/HMS Athinoula A. Martinos Center for Biomedical Imaging, Massachusetts General Hospital/Harvard Medical School, Charlestown, MA 02129, USA.

ABSTRACT

In optical coherence tomography (OCT), unbiased and low variance Doppler frequency estimators are desirable for blood velocity estimation. Hardware improvements in OCT mean that ever higher acquisition rates are possible. However, it is known that the Kasai autocorrelation estimator, unexpectedly, performs worse as acquisition rates increase. Here we suggest that maximum likelihood estimators (MLEs) that utilize prior knowledge of noise statistics can perform better. We show that the additive white Gaussian noise maximum likelihood estimator (AWGN MLE) has a superior performance to the Kasai autocorrelation estimate under additive shot noise conditions. It can achieve the Cramer-Rao Lower Bound (CRLB) for moderate data lengths and signal-to-noise ratios (SNRs). However, being a parametric estimator, it has the disadvantages of sensitivity to outliers, signal contamination and deviations from noise model assumptions. We show that under multiplicative decorrelation noise conditions, the AWGN MLE performance deteriorates, while the Kasai estimator still gives reasonable estimates. Hence, we further develop a multiplicative noise MLE for use under multiplicative noise dominant conditions. According to simulations, this estimator is superior to both the AWGN MLE and the Kasai estimator under these conditions, but requires knowledge of the decorrelation statistics. It also requires more computation. For actual data, the decorrelation MLE appears to perform adequately without parameter optimization. Hence we conclude that it is preferable to use a maximum likelihood approach in OCT Doppler frequency estimation when noise statistics are known or can be accurately estimated.

Keywords: Cramer-Rao bounds, maximum likelihood estimation, Doppler optical coherence tomography.

1. INTRODUCTION

With ever increasing acquisition speeds in traditional OCT systems,[1,2] and an increasing range of in-vivo applications, a one-size fits all approach to data analysis is no longer sufficient. In the area of Doppler frequency estimation for blood velocity determination, the noise regime and computational power available would determine the best algorithm to use. In this work we examine the statistical performance of frequency estimators[3–5] for use in Doppler optical coherence tomography (OCT),[6–8] under different noise assumptions. Under additive shot noise conditions, we show that the commonly used Kasai estimator is statistically sub-optimal, but can still perform adequately in the presence of moderate amounts of multiplicative decorrelation noise. The AWGN MLE, on the other hand, is statistically optimal and achieves the Cramer-Rao lower bound (CRLB) for moderate SNRs and data lengths. The downside of this optimality is that it is more sensitive to deviations from noise assumptions. Even small amounts of multiplicative decorrelation noise causes its performance to be worse than that of the Kasai estimator.[9] As decorrelation noise is commonly encountered for in-vivo situations in OCT, we derive a multiplicative decorrelation noise MLE that performs better than both the Kasai estimator and AWGN

Further author information: (Send correspondence to Edmund Y. Lam)
Aaron C. Chan: E-mail: cwachan@eee.hku.hk
Edmund Y. Lam: E-mail: elam@eee.hku.hk
Vivek J. Srinivasan: E-mail: vjsriniv@ucdavis.edu, vjsriniv@nmr.mgh.harvard.edu

Optical Coherence Tomography and Coherence Domain Optical Methods in Biomedicine XVII, edited by James G. Fujimoto, Joseph A. Izatt, Valery V. Tuchin, Proc. of SPIE Vol. 8571, 85712H
 · doi: 10.1117/12.2001188

MLE under conditions where multiplicative decorrelation noise is dominant. However, parametric methods such as maximum likelihood methods generally require more computation.

2. KASAI ESTIMATOR

Kasai derived an estimator[3] to calculate Doppler shifts of continuous wave ultrasound signals. While derived for processing analog signals, it is often utilized in its discrete form for OCT. The phase, $\angle$, of the lag one autocorrelation function acts as an estimate of the phase change during this time interval. From this one obtains an estimate for the Doppler frequency, given by

$$\hat{\Omega}_{\text{Kasai}} = \frac{\angle\left(\sum_{n=1}^{N-1} s_{n+1}s_n^*\right)}{\Delta t} = \frac{\angle\left\{\sum_{n=1}^{N-1} |s_{n+1}||s_n| \exp[j(\phi_{n+1}-\phi_n)]\right\}}{\Delta t}. \tag{1}$$

Here s_n is the signal acquired at the nth time instance, ϕ_n, its phase, and Δt, the time between measurements. As no assumptions are made about the noise statistics, the Kasai method provides reasonable estimates even in the presence of decorrelation noise (Fig. 3).[10] It therefore has a wider applicability than a parametric method such as the maximum likelihood estimator. However its non-parametric nature means that *a priori* knowledge of the noise statistics is not utilized, resulting in statistical sub-optimality. Its wide applicability comes at the price of optimality.

3. ADDITIVE WHITE GAUSSIAN NOISE MAXIMUM LIKELIHOOD ESTIMATOR

If s_n is a single measured datum at time instance n, we represent the Doppler OCT data for measuring flow velocity as

$$s_n = |r| \exp[j(n\Omega\Delta t + \phi_r)] + z_n. \tag{2}$$

Here, $|r| \exp(j\phi_r)$ is the unknown complex constant reflectance, and $j = \sqrt{-1}$. The time between measurements is $\Delta t = T/N$, where T is the total acquisition time and N is the total number of samples. The additive noise is given by z_n, which is circularly symmetric complex Gaussian. That is, each of the real and imaginary parts of z_n are independent and identically Gaussian distributed with zero mean and equal variance.

From this model, as expressed in (2), we can calculate the likelihood of obtaining a measured signal. If s_1 is a single measured datum, then each of the real and imaginary parts of the *complex* residual, $s_1 - |r| \exp[j(\Omega\Delta t + \phi_r)]$, will have a Gaussian distribution with zero mean and variance σ^2. Hence the likelihood is given by

$$\mathrm{P}\ (s_1|\,\Omega, \phi_r) = \frac{1}{2\pi\sigma^2} \exp\left\{ \frac{\left[x_1 - |r| \cos(\frac{n\Omega T}{N} + \phi_r)\right]^2 + \left[y_1 - |r| \sin(\frac{n\Omega T}{N} + \phi_r)\right]^2}{2\sigma^2} \right\} \tag{3}$$

where $x_1 = \mathrm{Re}[s_1]$ is the real part of the signal and $y_1 = \mathrm{Im}[s_1]$ is the imaginary part. By grouping the N datum together, the log-likelihood function for the data can then be written in the form,

$$L = \log\left[\mathrm{P}\ (\{s_1, s_2, \ldots, s_N\}|\Omega, \phi_r)\right] = -N \log(2\pi\sigma^2) \underbrace{- \frac{1}{2\sigma^2} \sum_{n=1}^{N} \left| s_n - |r| \exp\left[j \left(\frac{n\Omega T}{N} + \phi_r \right) \right] \right|^2}_{\text{variable term}}. \tag{4}$$

The first term is a constant, and the second term can be written as

$$-\sum_{n=1}^{N} \left(|s_n|^2 + |r|^2 \right) + 2 \sum_{n=1}^{N} \mathrm{Re}\left\{ s_n^* |r| \exp\left[j \left(\frac{n\Omega T}{N} + \phi_r \right) \right] \right\}, \tag{5}$$

the last term of which is the real part of inverse discrete Fourier transform of $\{s_1^*, \ldots, s_N^*\}$. The AWGN MLE, $\hat{\Omega}_{\text{MLE}}$, is obtained by choosing the values of the Doppler frequency, Ω, and reflectance phase, ϕ_r, that maximizes the real part of the inverse DFT of the (complex conjugate of the) signal,[5]

$$(\hat{\Omega}_{\text{MLE}}, \hat{\phi}_{\text{MLE}})^T = \underset{\mathbf{\Omega}, \phi_\mathbf{r}}{\arg\max} \left(\mathrm{Re}\left\{ |r| \sum_{n=1}^{N} s_n^* \exp\left[j \left(\frac{n\Omega T}{N} + \phi_r \right) \right] \right\} \right). \tag{6}$$

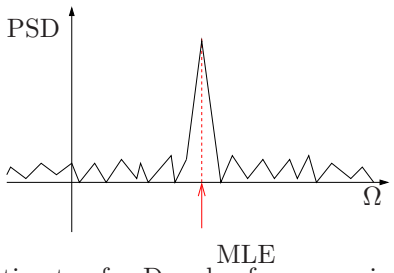

Figure 1: The maximum likelihood estimator for Doppler frequency is the location of the peak of the power spectral density.

As ϕ_r is chosen to make the expression in curly brackets real, this is equivalent to finding the frequency corresponding to the peak of the power spectral density. As the AWGN MLE is parametric, provided that the acquired signal is well described by the noise model, it is asymptotically efficient and unbiased. However, its performance may deteriorate in the presence of outliers or deviations from model assumptions, such as in the presence of decorrelation noise.

4. MULTIPLICATIVE DECORRELATION MAXIMUM LIKELIHOOD ESTIMATOR

Consider a stationary OCT beam such that a voxel is imaging a transverse blood vessel. At any time instant, there are scatterers randomly distributed within the voxel. As the scatters move into and out of a voxel, the signal "decorrelates." This causes relaxation of the auto-covariance function. One can simulate decorrelation with Doppler shifted correlated random variables. Hence the signal is obtained by modifying the signal from (2) to include a multiplicative term q_n,

$$s_n = q_n |r| \exp[j(n\Omega\Delta t)] + z_n, \tag{7}$$

where q_n is a correlated complex Gaussian random variable with a known auto-covariance matrix, $\mathbf{\Sigma}$. Here $\mathbf{\Sigma}$ is real and Toeplitz symmetric, with the first row (the auto-covariance function) having a Gaussian profile. Its $1/e$ full-width is determined by the coherence time of the signal. Defining

$$\bar{\mathbf{S}} = \begin{pmatrix} \mathrm{Re}[s_1 \exp(-j\Omega\Delta t)] & \dots & \mathrm{Re}[s_N \exp(-jN\Omega\Delta t)] & \mathrm{Im}[s_1 \exp(-j\Omega\Delta t)] & \dots & \mathrm{Im}[s_N \exp(-jN\Omega\Delta t)] \end{pmatrix}^T, \tag{8}$$

the $2N$ by $2N$ covariance matrix by $\bar{\mathbf{\Sigma}} = \begin{pmatrix} \mathbf{\Sigma} & \mathbf{0}_N \\ \mathbf{0}_N & \mathbf{\Sigma} \end{pmatrix}$, and setting $z_n = 0$, the likelihood function is then given by,

$$\mathrm{P}\left(\{s_1, \dots, s_N\} | \, \Omega\right) = \frac{1}{(2\pi)^N \det\left(\bar{\mathbf{\Sigma}}\right)^{\frac{1}{2}}} \exp\left(-\frac{1}{2}\bar{\mathbf{S}}^T \bar{\mathbf{\Sigma}}^{-1} \bar{\mathbf{S}}\right). \tag{9}$$

Therefore the multiplicative decorrelation MLE for Ω is

$$\hat{\Omega}_{\mathrm{dMLE}} = \arg\min_{\Omega} \left(\bar{\mathbf{S}}^T(\Omega) \bar{\mathbf{\Sigma}}^{-1} \bar{\mathbf{S}}(\Omega)\right). \tag{10}$$

Maximizing the log-likelihood is equivalent to minimizing the quadratic form $\bar{\mathbf{S}}^T(\Omega)\bar{\mathbf{\Sigma}}^{-1}\bar{\mathbf{S}}(\Omega)$ with respect to Ω. This can be computed using standard optimization algorithms.[11]

5. AWGN CRAMER-RAO LOWER BOUND

The theoretical best performance of an unbiased estimater is given by the Cramer-Rao Lower Bound(CRLB). The CRLB for an estimator assuming additive white Gaussian noise (AWGN) is given by,[5]

$$\mathrm{Var}\left(\hat{\theta}_1\right) = \mathrm{Var}\left(\hat{\Omega}\right) \geq \frac{12N\sigma^2}{(N^2-1)|r|^2 T^2}. \tag{11}$$

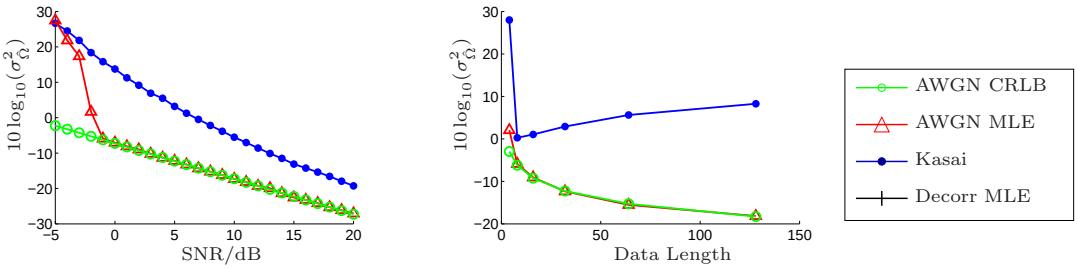

(a) (b)

Figure 2: (a) Estimator performance in the presence of AWGN, for a data length of $N = 32$, an acquisition time of $T = 1$ ms, and SNR of 5 dB. Lower is better. Variances are measured in krad^2.s^{-2}. The AWGN MLE achieves the CRLB except for at low SNRs.
(b) MSE of Kasai estimator and AWGN MLE against data length for a constant acquisition time of $T = 1$ ms and SNR of 5 dB. Maintaining a constant SNR while increasing the acquisition rate would require increasing the detected photon rate (power).

For large N, the CRLB can be approximated as,

$$\mathrm{Var}_{\mathrm{CR}}(\hat{\Omega}) \approx \frac{12\sigma^2}{N|r|^2T^2}. \tag{12}$$

Here the CRLB, for large N, is inversely proportional to the total number of samples, N. It is also inversely proportional to the SNR, $|r|^2/2\sigma^2$, and inversely proportional to the square of the total acquisition time T. Further insight can be achieved by assuming a constant rate of detected photons (power). With this assumption the shot-noise limited SNR is proportional to $\Delta t = T/N$. Under these conditions,

$$\mathrm{Var}_{\mathrm{CR}}(\hat{\Omega}) \sim 1/T^3. \tag{13}$$

Thus, if the number of samples is sufficiently large, the SNR is shot noise limited, and the rate of detected photons (power) is constant, the CRLB has the intuitive property of being inversely proportional to the cube of the total acquisition time. This can be understood intuitively, as the total number of photons detected is proportional to T, while an additional factor of $1/T^2$ arises because the variance of the spectrum is proportional to $1/T^2$. More importantly for large N, the CRLB becomes independent of N. As the MLE variance approaches the CRLB asymptotically, we can infer that for sufficiently large N, the MLE variance also becomes independent of sampling rate. This behavior contrasts with the Kasai estimator, whose variance increases with increasing sampling rate.

6. COMPARISON OF PERFORMANCE BY SIMULATION

We ran simulations to estimate the variances and biases of the estimators. The analog frequency was assumed to be $\Omega = 3\pi \times 10^3$ rad.s^{-1} for all simulations. We define the SNR to be $|r|^2/2\sigma^2$. Fig. 2 shows that for a data length of $N = 32$, under shot noise conditions, the AWGN MLE achieves the CRLB with the SNR roughly at -1 dB. The Kasai estimator slowly approaches the CRLB with increasing SNR, but is worse than the CRLB by more than 7 dB. Fig. 2b shows that the MSE of the Kasai estimator increases with increasing acquisition rate, when the SNR is kept constant. This is also true if the detected photon rate (power) is kept constant.[5] This is non-intuitive and unexpected behavior, since one would expect that increasing the sampling rate would provide more information about parameters to be estimated. Sometimes the Kasai lag can be increased to achieve a more precise Kasai estimate, but this has the undesirable consequence of decreasing the maximum measurable Doppler frequency. Moving scatterers also introduce multiplicative decorrelation noise into the signal. Fig. 3 shows that under the presence of multiplicative noise, and negligible additive noise, the decorrelation noise MLE has the best performance except for at very low acquisition rates, and the AWGN MLE performance deteriorates.

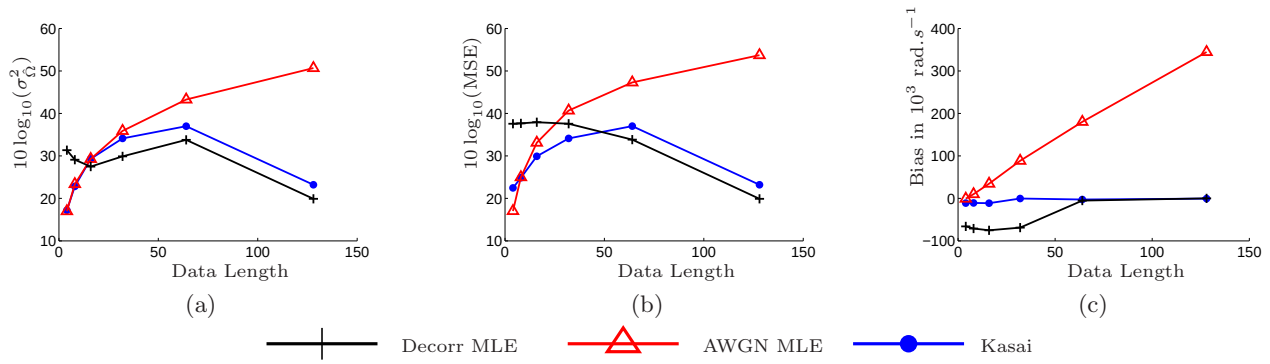

Figure 3: (a) Estimators under multiplicative decorrelation noise and negligible additive noise. The acquisition time is 1 ms. The $1/e$ full-width coherence time is 0.01 ms. Variances are measured in krad^2.s^{-2}. Here, the AWGN MLE performs the worst.
(b) Mean squared error. (c) Estimator bias in thousands of radians per second.

7. EXPERIMENTAL VERIFICATION

7.1 System Description

A 1310 nm spectral/Fourier domain OCT microscope was used for the imaging of a flow phantom. The light source consisted of two superluminescent diodes combined by using a 50/50 fiber coupler to yield a spectral bandwidth of 170 nm. The axial (depth) resolution was 3.6 μm, full-width-at-half-maximum, and the transverse resolution was 7.2 μm (full-width-at-half-maximum), and the highest imaging speed was 47000 axial scans per second, achieved by an InGaAs line scan camera (Goodrich-Sensors Unlimited, Inc.). The camera sensitivity was typically set to "medium" to obtain the widest dynamic range. The high sensitivity setting typically resulted in a signal saturating the camera pixels. A 5× objective, Mitsutoyu, was used and the center of tubing was placed in focus.

7.2 Intralipid Flow Phantom

We used Intralipid-10%[12] and a syringe pump with 0.58 mm diameter tubing. Intralipid globules have an average diameter of 100 nm. The pipe was placed at a 16 degree incline, so that there was an axial velocity which could be measured as a Doppler shift. Fluid flow in a tube has a Poiseuille profile, hence measurements of the Doppler shift were taken at 0.16 mm from the inner edge of the tubing. Fig. 4 shows that for a 9.0 ml.hr^{-1} flow rate, the Kasai estimator had the best performance, followed by the decorrelation MLE, and then the AWGN MLE. To reduce computational time for the decorrelation noise MLE, the Kasai estimates were taken as the starting values for the minimization in eq. (10), and the search domain was restricted to three Kasai estimate standard deviations above and below this value. To compute the decorrelation MLE, an auto-covariance function consisting of a sum of an exponential decay and a Gaussian function was used. This function was chosen to approximate the shape of the experimentally obtained autocorrelation function. The full-width $1/e$ maximum was set to 0.255 ms for the exponential function and 0.51 ms for the Gaussian function. The DFT length of the AWGN MLE was increased by 256 times using zero padding, so that the estimator variance would not be artifactually rounded to zero.

In this regime, there is a significant amount of decorrelation noise. The effects of decorrelation, one of which is to reduce the SNR, are negligible if acquisition time is less than the coherence time of the signal, but increase as acquisition times increase. Hence the decorrelation MLE performed better than the AWGN MLE. However, to achieve a performance better than the Kasai estimator, more parameter fine tuning with regards to the shape of the input auto-covariance function is required. Other sources of noise such as galvanometer jitter, thermal drift, and other phase instabilities, could also contribute to a worse performance.

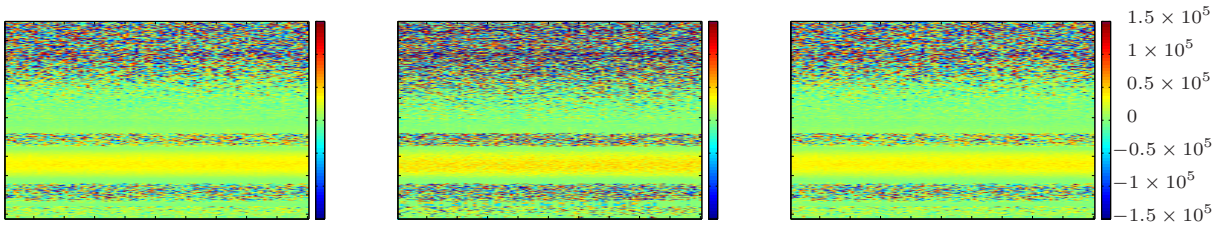

(a) (b) (c) (Measurements in rad.s^{-1})

Figure 4: Color Doppler Maps of 9ml.hr^{-1} intralipid flow. The tubing width is 0.58 mm. Estimates were made from data vectors of length 128. The OCT line scan rate was rate was 47 kHz. As only a line scan was taken, the x-axis represents a time axis. (a) The Kasai estimator variance was 4.2 krad^2.s^{-2} (6.2 dB). (b) The AWGN MLE variance was 63.1 krad^2.s^{-2} (18 dB). (c) The decorrelation MLE variance was 13.0 krad^2.s^{-2} (11.1 dB).

8. CONCLUSION

In this work we have discussed and demonstrated the relative advantages and deficiencies of the Kasai autocorrelation estimator. While it has reasonable performance and wide applicability due to its non-parametric nature, it is not optimal: neither in shot noise dominant nor in multiplicative decorrelation noise dominant conditions, as prior knowledge of noise statistics is not utilized. We have shown with simulation that the AWGN MLE is statistically optimal under additive white Gaussian noise conditions, but is sensitive to multiplicative decorrelation noise. Simulations also show that, under decorrelation noise dominant conditions, the decorrelation noise MLE performs better than the Kasai estimator.

Experimental results confirm that the decorrelation MLE performs better than the AWGN MLE in flow phantom situations. However, without parameter optimization, its performance is slightly worse than that of the Kasai estimator. It is possible that other sources of noise, or flow instabilities are contributing to a perceived lower estimation performance. Despite this, the decorrelation noise MLE still performs adequately. More optimization is required to improve the performance of the decorrelation noise MLE. In particular, the shape of the autocovariance function can be tweaked to better match experimental situations. With further development, we expect that it would be preferable to use a maximum likelihood approach in OCT Doppler frequency estimation when noise statistics are known or can be accurately estimated.

With further refinement we expect that MLE estimators can reach the theoretical performance levels required for in-vivo applications. The type of imaging device and its specific application will determine the appropriate algorithm for Doppler frequency estimation. In the absence of knowledge of the noise statistics, the Kasai algorithm would provide a good first estimate. More sophisticated algorithms, such as our decorrelation MLE would be suited to systems with high acquisition rates and where the noise statistics are known. Although more computationally intensive, MLEs make use of prior knowledge of the noise statistics and can deliver better estimation performance.

9. ACKNOWLEDGMENT

We acknowledge support from the University Research Committee of the University of Hong Kong under Project 10401797, the National Institutes of Health (R00NS067050, EB001954 R01), the American Heart Association (11IRG5440002), and the Glaucoma Research Foundation Catalyst for a Cure. We also thank Maria Angela Franceschini for permission to use the OCT system.

REFERENCES

[1] Wojtkowski, M., Srinivasan, V., Ko, T., Fujimoto, J., Kowalczyk, A., and Duker, J., "Ultrahigh-resolution, high-speed, fourier domain optical coherence tomography and methods for dispersion compensation," *Opt. Express* **12**, 2404–2422 (May 2004).

[2] Srinivasan, V. J., Jiang, J. Y., Yaseen, M. A., Radhakrishnan, H., Wu, W., Barry, S., Cable, A. E., and Boas, D. A., "Rapid volumetric angiography of cortical microvasculature with optical coherence tomography," *Opt. Lett.* **35**, 43–45 (January 2010).

[3] Kasai, C., Namekawa, K., Koyano, A., and Omoto, R., "Real-time two-dimensional blood flow imaging using an autocorrelation technique," *IEEE Trans. Sonics Ultrason.* **32**, 458–464 (May 1985).

[4] Loupas, T., Powers, J., and Gill, R., "An axial velocity estimator for ultrasound blood flow imaging, based on a full evaluation of the doppler equation by means of a two-dimensional autocorrelation approach," *IEEE Trans. Ultrason. Ferroelectr. Freq. Control* **42**, 672–688 (July 1995).

[5] Chan, A. C., Lam, E. Y., and Srinivasan, V. J., "Comparison of kasai autocorrelation and maximum likelihood estimators for doppler optical coherence tomography," *IEEE Trans. Med. Imag., (in submission)* (2013).

[6] Szkulmowski, M., Szkulmowska, A., Bajraszewski, T., Kowalczyk, A., and Wojtkowski, M., "Flow velocity estimation using joint spectral and time domain optical coherence tomography," *Opt. Express* **16**, 6008–6025 (April 2008).

[7] Szkulmowska, A., Szkulmowski, M., Kowalczyk, A., and Wojtkowski, M., "Phase-resolved doppler optical coherence tomography—limitations and improvements," *Opt. Lett.* **33**, 1425–1427 (July 2008).

[8] Schmoll, T., Kolbitsch, C., and Leitgeb, R. A., "Ultra-high-speed volumetric tomography of human retinal blood flow," *Opt. Express* **17**, 4166–4176 (March 2009).

[9] Chan, A. C., Lam, E. Y., and Srinivasan, V. J., "Optimal doppler frequency estimators for ultrasound and optical coherence tomography," in [*2012 IEEE BioCAS Conference*], (November 2012).

[10] Vakoc, B., Tearney, G., and Bouma, B., "Statistical properties of phase-decorrelation in phase-resolved doppler optical coherence tomography," *IEEE Trans. Med. Imag.* **28**, 814–821 (June 2009).

[11] Forsythe, G. E., Malcolm, M. A., and Moler, C. B., [*Computer Methods for Mathematical Computations*], Prentice-Hall (1976).

[12] van Staveren, H., Moes, C., van Marle, J., Prahl, S., and van Gemert, M., "Light-Scattering in Intralipid-10-Percent in the Wavelength Range of 400-1100 NM," *Appl. Opt.* **30**, 4507–4514 (November 1991).